

Ag/GaP nanoparticles with photooxidation property under visible light

Zhao-Chun Zhang · Jian-Lin Li

Received: 24 October 2010 / Accepted: 12 January 2011 / Published online: 25 January 2011
© Springer Science+Business Media, LLC 2011

Abstract This article reports the use of Gallium phosphide (GaP) and Ag/GaP nanoparticles, which can harness visible light to decompose organic dye in aqueous solution. The Ag(1.139 wt%)/GaP and Ag(5.225 wt%)/GaP nanoparticles were prepared by the liquid phase reduction of silver nitrate with hydrazine hydrate. The application of X-ray fluorescence and high-resolution transmission electron micrograph morphology has provided direct evidence of the presence of silver on the GaP nanoparticles. Under visible light, the experiments on the photocatalytic degradation of crystal violet in solution over the GaP and Ag/GaP nanoparticles were carried out. The results reveal that small size and number density of Ag domains deposited on GaP nanoparticles have enhanced photocatalytic efficiencies, as compared to large size and number density of Ag domains. This study suggests the potential of both GaP and Ag/GaP nanoparticles as photofunctional materials for waste-water cleaning.

Introduction

Gallium phosphide (GaP) is an important semiconductor material with indirect band gap ($E_{g,ind} = 2.272$ eV, 300 K) [1]. The temperature and pressure dependences of $E_{g,ind}$ for GaP crystal are $dE_{g,ind}/dT = -5.2 \times 10^{-4}$ eV K⁻¹ [2] and $dE_{g,ind}/dp = -1.4 \times 10^{-6}$ eV/kg cm⁻² [3], respectively. There has been intense interest in studying GaP nanomaterials, particularly dots, rods, wires, belts, trees and related

structures, because of the potential applications in optoelectronics [4–15]. Much work laid the emphasis on the studies examining the morphology and characterization of GaP nanomaterials. However, little literature is available on the photocatalytic and photoelectrocatalytic properties of GaP nanomaterials.

Photocatalytic efficiency can be expressed quantitatively by quantum yield, which is diversely proportional to the sum of transfer rate and recombination rate of photoinduced charged carriers. So far, many approaches have been explored to control the recombination rate of charged carriers and to enhance the visible light response of wide band gap (UV-active) photocatalysts. The deposition of noble metals onto photocatalyst surfaces is an effective way of enhancing photocatalyst activity. It has been proved that an appropriate number density of Pt deposits on TiO₂ can lead to increase in charge carrier separation distance and to decrease in charge carrier recombination [16]. Supported Ag nanoclusters are often used for applications in photocatalysis [17–22].

As part of systematic study of the optoelectronic characteristic of GaP nanoparticles [23–26], in the current research the photocatalytic activities of GaP nanoparticles and Ag/GaP composite nanoparticles under visible light were investigated.

Experimental

Synthesis of Ag/GaP nanoparticles

GaP nanoparticles are synthesized by the reaction of anhydrous gallium (III) chloride (GaCl₃) with sodium phosphide (Na₃P) in dimethylbenzene at 373 K. The detailed synthetic procedure was reported originally elsewhere [26], therefore,

Z.-C. Zhang (✉) · J.-L. Li
School of Material Science and Engineering,
Shanghai University, Shanghai 200072, China
e-mail: zhangzhaochun@shu.edu.cn

no modification of that procedure to prepare the GaP nanoparticles will be described here.

The Ag/GaP nanoparticles, theoretical wt% Ag of 1 and 5%, respectively, were prepared from suspensions of 1 g of as-prepared GaP nanoparticles in 20 mL of water, plus appropriate volumes of 0.1 mol L⁻¹ AgNO₃. These slurries were magnetically stirred for 6 h. Then, 0.5 mL of 50% hydrazine hydrate (N₂H₄·H₂O) solution were added slowly with continuous, rapid stirring for 6 h. The suspensions were filtered, washed with water, and the solid photocatalysts dried in an oven maintained at 323 K.

Characterizations of GaP and Ag/GaP nanoparticles

The GaP and Ag/GaP nanoparticles were characterized by X-ray diffraction (XRD) using an X-ray diffractometer (D/max-rC) with nickel-filtered Cu K α radiation. A XRF-1800 X-ray fluorescence (XRF) spectrometer was used in the identification of Ag element and quantitative analysis. High-resolution transmission electron micrograph (HRTEM) images were recorded on a JEM-2010F microscope operated at 200 kV. Fluorescence spectrum of the GaP nanoparticles was measured on a fluorescence spectrophotometer (F-7000 FL) using Xe lamp with excitation wavelength of 300 nm at room temperature. Diffuse reflectance measurements on optically thick GaP and Ag/GaP nanoparticles were collected using a Shimadzu Spectrometer UV-2501 PC. Barium sulfate (BaSO₄) was chosen as the reference standard.

Photocatalytic reactor and procedures

The main experimental setup is comprised of a cylindrical 120 mL glass water jacketed static reactor, a 300 W Xe lamp with an UV cutoff filter (providing visible light with $\lambda > 420$ nm) mounted 35 cm above the water-cooled jacket of the reactor. Photocatalytic degradation of crystal violet (C₂₅H₃₀ClN₃) in the aqueous solution was performed with 0.060 g of the GaP or Ag/GaP nanoparticles suspended in 30 mL of crystal violet solution at room temperature and normal atmosphere pressure. The initial concentration of crystal violet was 2.70 × 10⁻⁵ mol L⁻¹. At any given irradiation time interval, the dispersion was continuously stirred, sampled (5 mL), and centrifuged to separate the GaP or Ag/GaP nanoparticles. The supernatant liquid was monitored by the absorbance at 610 nm with an UV/Vis spectroscopy. The photocatalytic degradation ratio, D , of crystal violet is given by

$$D = \frac{C_0 - C_t}{C_0} \times 100\% \quad (1)$$

where C_0 is the concentration of crystal violet initially (at $t = 0$), C_t is the concentration at a later time t .

Results and discussion

XRF and XRD analyses of Ag/GaP nanoparticles

The elemental analysis by microprobe X-ray fluorescence indicates that two Ag/GaP samples contain 1.139 and 5.225 wt% Ag, respectively.

Figure 1 shows the X-ray diffraction spectra of the Ag(1.139 wt%)/GaP and Ag(5.225 wt%)/GaP nanoparticles, respectively. The (hkl) values assigned to peaks corresponding to the cubic GaP and Ag are in agreement with standard JCPDS values (GaP: 80-0015; Ag: 04-0783). The XRD pattern of the Ag(1.139 wt%)/GaP nanoparticles show no presence of Ag. This arises mainly because XRD procedures are less successful in identifying Ag deposits on the GaP nanoparticles, where the nominal wt% Ag ranges from 0 to 2%.

TEM analysis of GaP and Ag/GaP nanoparticles

Representative TEM micrographs of the GaP and Ag/GaP nanoparticles are given in Fig. 2. It can be seen that the GaP nanoparticles are not spherical, but ellipsoidal to some extent with serious mutual aggregation. Roughly, the equivalent diameter ranges from about 15 to 35 nm. The typical HRTEM image of the Ag(1.139 wt%)/GaP nanoparticles reveals that many small Ag clusters (several nanometer in diameter) are attached to the surface of the GaP nanoparticles, in addition to the large Ag nanoparticles located nearby. By contrast, for the Ag(5.225 wt%)/GaP nanoparticles the small Ag clusters disappear and more large Ag nanoparticles are observed. The Ag nanoparticles are subglobular in shape. A careful observation of the typical images suggests that the Ag domains of both

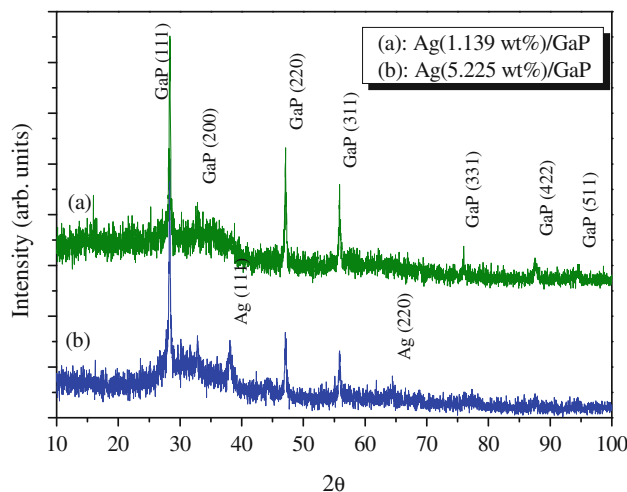


Fig. 1 X-ray diffraction spectra of Ag(1.139 wt%)/GaP (a) and Ag(5.225 wt%)/GaP (b) nanoparticles

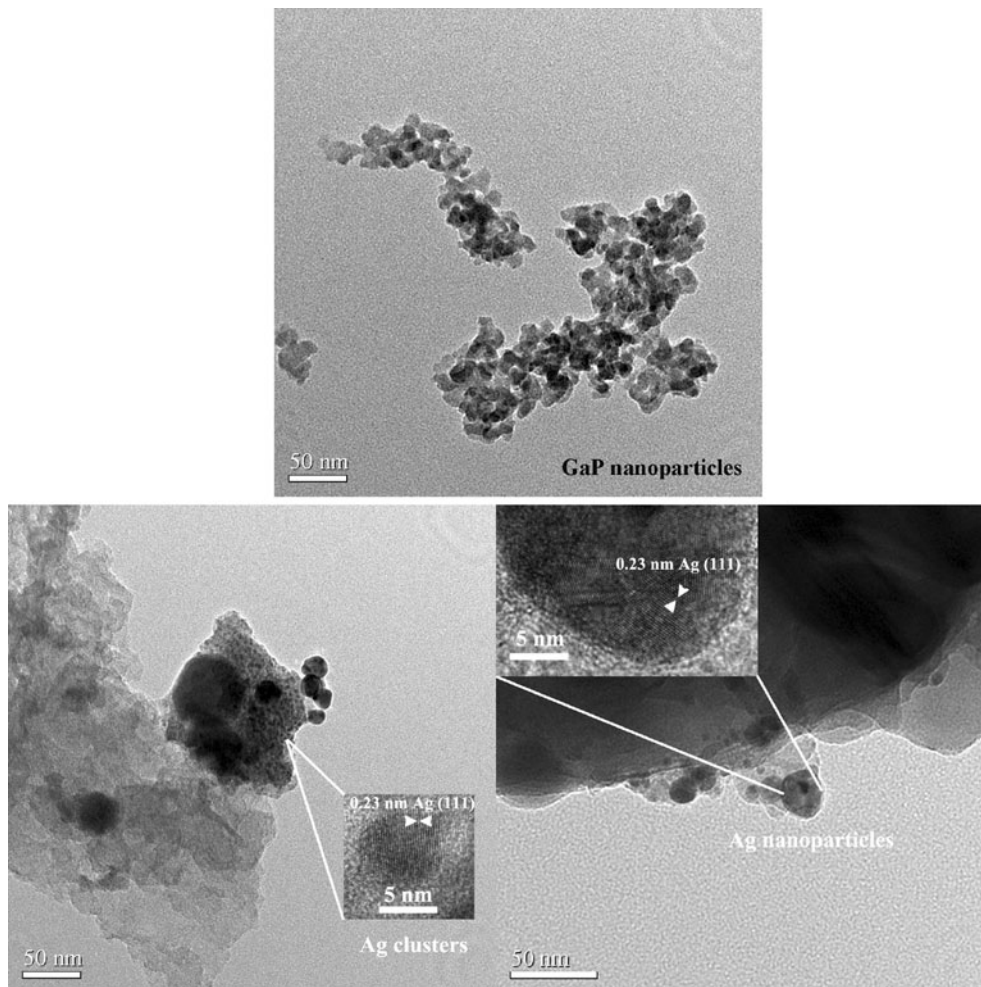


Fig. 2 TEM micrographs of GaP and Ag/GaP nanoparticles

Ag(1.139 wt%)/GaP and Ag(5.225 wt%)/GaP samples are not well-distributed on the surface of the GaP nanoparticle aggregates. It seems that the Ag clusters and Ag nanoparticles are inclined to deposit together on some certain micro-regions. Taking account of the fact that the wt% Ag of Ag(5.225 wt%)/GaP is greater than that of Ag(1.139 wt%)/GaP by approximately five times, it appears that the number density of Ag domains on GaP of Ag(5.225 wt%)/GaP can exceed significantly that of Ag(1.139 wt%)/GaP.

Fluorescence spectrum of GaP nanoparticles

Figure 3 shows the room temperature fluorescence spectrum of the GaP nanoparticles. An outstanding feature is that four emitting bands, including a strong blue emission centered at around 2.64 eV, one weak blue band centered at around 2.74, and two broad violet bands centered at around 3.00 and 3.10 eV, respectively, have been observed. The origin of two broad violet emissions can be attributed to the direct, momentum-conserving transitions

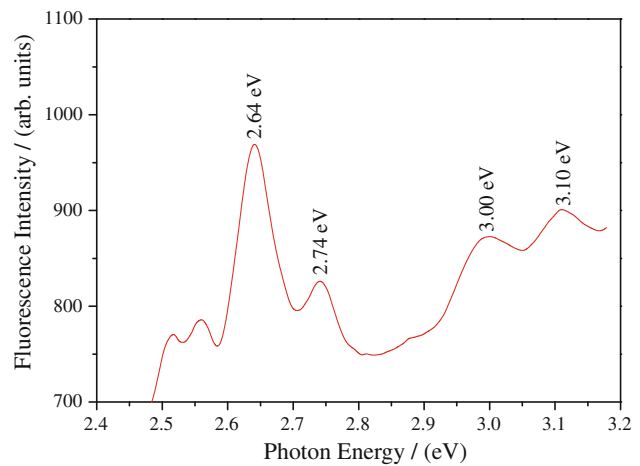


Fig. 3 Fluorescence of GaP nanoparticles at room temperature

near the Γ point of the Brillouin zone between the Γ_1 conduction band state and Γ_{15} valence band, that is, $\Gamma_{6c} - \Gamma_{8v}$ (3.00 eV) and $\Gamma_{6c} - \Gamma_{7v}$ (3.10 eV), respectively.

The origin of two blue emissions (2.74 and 2.64 eV) can be attributed to the indirect transitions between the X_1 conduction band state and Γ_{15} valence band, that is, $\Delta_{5c} - \Gamma_{8v}$ (2.64 eV) and $\Delta_{5c} - \Gamma_{7v}$ (2.74 eV), respectively.

UV–Vis diffuse reflectance spectra of GaP and Ag/GaP nanoparticles

The radiation transfer through a scattering and absorbing nonhomogeneous medium can be described by the equation of radiative transfer (ERT). There are various theories leading to an approximate solution of the ERT [27, 28]. The loose layers investigated in this article have the thickness on the order of millimeter and therefore exhibit nonisotropic scattering preferentially directed forward. The incident radiation of the spectrometer belongs to directional illumination. Consequently, the three-flux approximation was used instead to analytically solve the ERT. The three-flux approximation results in the following relation between the diffuse reflectance, R_∞ , of a directional illuminated, isotropically scattering, optically thick sample and the ratio of absorption coefficient to scattering coefficient, E_a/E_s

$$\frac{E_a}{E_s} = \frac{6}{5(R_\infty + 4)} \times \frac{(1 - R_\infty)^2}{2R_\infty} \quad (2)$$

The measured diffuse reflectance of optically thick samples and the ratio E_a/E_s calculated by using the three-flux approximation (Eq. 2) of the GaP and Ag/GaP nanoparticles are shown in Figs. 4 and 5, respectively.

It is clear from Figs. 4 and 5 that the reflectance and the ratio E_a/E_s difference between the GaP and Ag(1.139 wt%)/GaP nanoparticles is not sharp. There is little, if any,

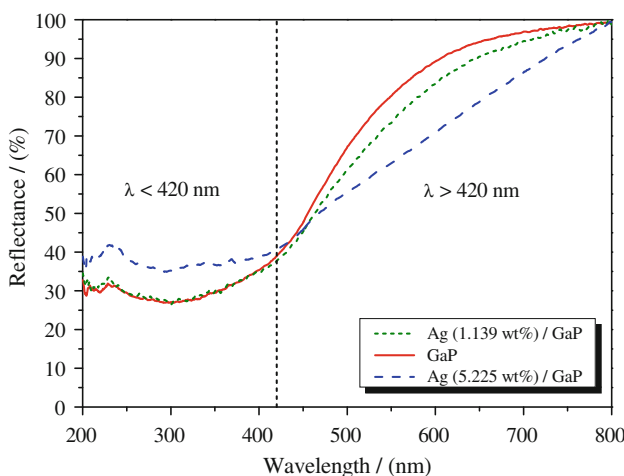


Fig. 4 Diffuse reflectance spectra of GaP and Ag/GaP nanoparticles. In the present photocatalytic experiment, an UV cutoff filter providing visible light with $\lambda > 420$ nm was used

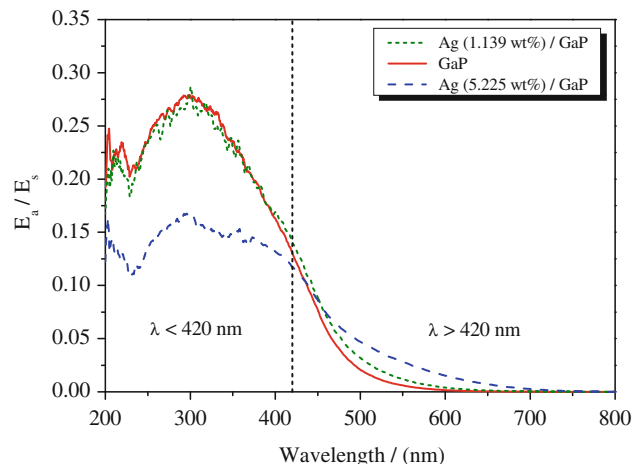


Fig. 5 Ratio E_a/E_s versus wavelength of GaP and Ag/GaP nanoparticles

difference between them. In contrast to this, the apparent reflectance or the ratio E_a/E_s difference lies between the GaP and Ag(5.225 wt%)/GaP nanoparticles. For the GaP and Ag/GaP nanoparticles, scattering is the dominate effect of radiation attenuation ($E_a/E_s < 1$). In the wavelength range from about 450 to 800 nm, the absorption of the Ag/GaP nanoparticles is enhanced to a small extent, because of the plasmon resonance of Ag. In other words, the ratio E_a/E_s of the Ag/GaP nanoparticles increases with increasing the Ag coverage. However, by comparison with the GaP nanoparticles, the absorption of the Ag(5.225 wt%)/GaP nanoparticles is decreased to some extent in the ultraviolet region. The high Ag coverage impedes the absorption of the GaP nanoparticles.

Photocatalytic activity of GaP and Ag/GaP nanoparticles under visible light

On the basis of the experimental procedures described above in “Photocatalytic reactor and procedures”, the photocatalytic degradation of crystal violet in aqueous solutions was investigated. Before illumination, the suspensions were magnetically stirred in the dark for ~ 30 min to ensure establishment of an absorption/desorption equilibrium of the dye on the sample surfaces. As the irradiation time increases, the decomposition of the dye over the GaP or Ag/GaP nanoparticles progresses, as showed in Fig. 6. In view of the fact that crystal violet can harvest visible light, experiment with the dye decomposition under visible light irradiation condition without the GaP and Ag/GaP nanoparticles was carried out. In the experiment, the dye concentration remained unchanged as a function of time, indicating that the GaP and Ag/GaP nanoparticles are the photocatalysts responsible for the dye degradation under visible light.

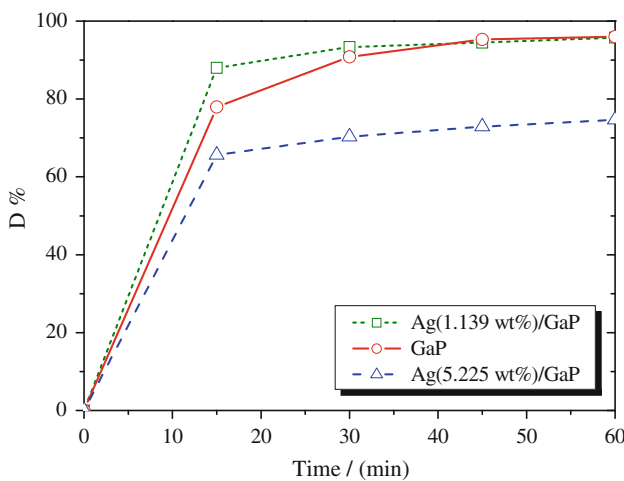


Fig. 6 Irradiation time dependence of photocatalytic degradation ratio of crystal violet in solution over GaP and Ag/GaP nanoparticles under visible light

It was found from Fig. 6 that under visible light irradiation the photocatalytic degradation ratio of crystal violet over the Ag(1.139 wt%)/GaP nanoparticles was approximately 1.13 times higher than that over the GaP nanoparticles, while the Ag(5.225 wt%)/GaP nanoparticles provided a lower photocatalytic degradation ratio of crystal violet, i.e., 1.19 times lower than the GaP nanoparticles in 15 min reaction. The photocatalytic degradation ratio of crystal violet over the GaP and Ag(1.139 wt%)/GaP nanoparticles reached above 95% in 60 min reaction, but that over the Ag(5.225 wt%)/GaP nanoparticles was limited within 80%, which confirmed that the Ag(5.225 wt%)/GaP nanoparticles had a worse photocatalytic activity.

The conduction band edge energy of GaP at the point of zero charge (E_{cs}^0) can be calculated by [29]

$$E_{\text{cs}}^0 = E^e - X + 1/2E_g \quad (3)$$

where E^e is the energy of free electrons on the hydrogen scale (≈ 4.5 eV), X is the electronegativity, and E_g is the energy band gap. The electronegativity of GaP can be calculated as the geometric mean of the electronegativities of Ga and P atoms. The atomic electronegativity is also given by the Mulliken definition, that is, the arithmetic mean of the atomic electron affinity and the first ionization energy. The energy band gap of the GaP nanoparticles is 2.64 eV, as indicated in Fig. 3. Substitution of this value into Eq. 3 with $X(\text{GaP}) = 4.24$ gives $E_{\text{cs}}^0 = 1.58$ eV.

Figure 7 shows the positions of the top of the GaP valence band and bottom of conduction band relative to the vacuum level of 0, combined with the relative positions of the work function of bulk Ag and a single atom of Ag, based on electron affinity measurements. The electron affinity of a gas phase Ag atom is reported to be 1.302 eV below vacuum level [30], placing the ground state of

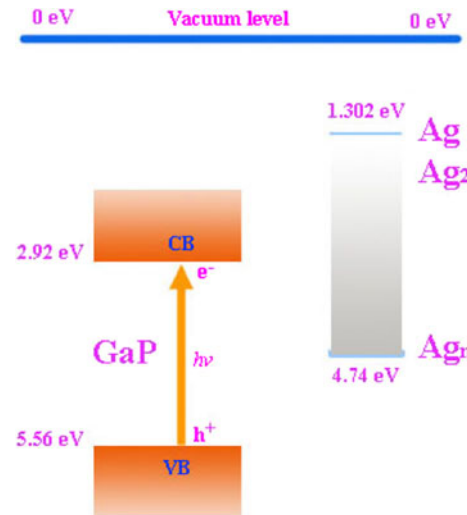
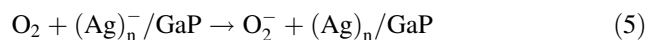


Fig. 7 Schematic diagram showing relative positions of top of valence band and bottom of conduction band of GaP nanoparticles, and work functions of bulk Ag and a single atom of Ag

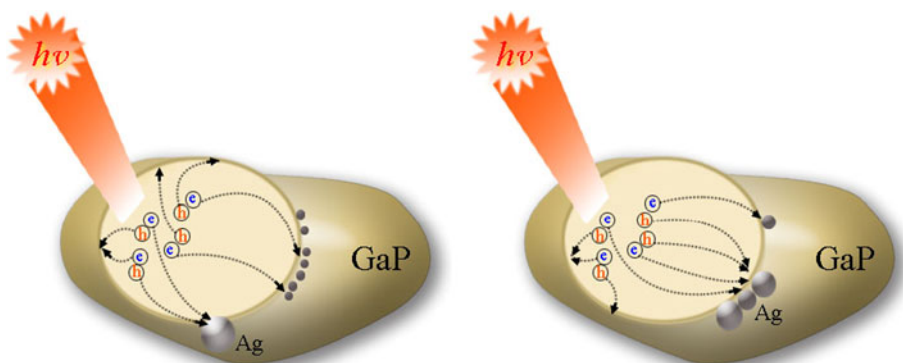
Ag^- well above the bottom of the GaP conduction band ($= -X + 1/2E_g = -2.92$ eV). The literature value for the work function of bulk Ag is reported to be 4.74 eV below vacuum level [31], positioning it within the GaP band gap (top of valence band = $-2.92 - 2.64 = -5.56$ eV). Based on these energy levels, as shown in Fig. 7 for Ag/GaP system, it appears that small Ag clusters on GaP are capable of accepting photoelectrons from the bottom of GaP conduction band. Large Ag nanoparticles, however, are considered to function as recombination sites, based on their ability to capture both photoelectrons and holes.

Gerisher [32] has pointed out the importance of the rate of oxygen (O_2) reduction by photoinduced electrons in preventing recombination of the photoinduced charge carriers during photocatalytic processes utilizing semiconductor particles, and suggested that the superoxide radical ion (O_2^-) formation might be the slowest step in the photocatalytic processes resulting in the oxidation of organic molecules by $\cdot\text{OH}$ radicals or directly by photoinduced holes. For the Ag(1. wt%)/GaP nanoparticles, a major role of surface deposition of Ag clusters is attributed to acceleration of O_2^- formation, with the effect of decreasing recombination of photoinduced charge carriers and increasing product yields initiated by photoinduced holes or $\cdot\text{OH}$ radicals.



But for the Ag(5.225 wt%)/GaP nanoparticles, as the number and size of the Ag nanoparticles become large, the silver deposits may begin to function as recombination centers of the photoinduced charge carriers and the

Fig. 8 Schematic diagrams showing effect of size and number density of Ag deposits on GaP in decreasing recombination of photoinduced charged carriers: *left* small size and low number density of Ag deposits resulting in decrease in charge carrier recombination, as compared to GaP nanoparticles in absence of Ag; *right* large size and high number density of Ag deposits resulting in increase in charge carrier recombination



advantages of the metallic deposition are lost. For large size and number density of Ag domains on GaP, reaction (6) competes with reaction (5).



Consequently, large size and number density of Ag domains are considered to function as recombination sites, based on their ability to capture both photoinduced electrons and holes. This is shown schematically in Fig. 8.

Gerisher's comments are consistent with the photocatalytic degradation of crystal violet in solution over the Ag/GaP nanoparticles of the present investigation. Here, the photocatalytic degradation ratio of crystal violet over the Ag(1.139 wt%)/GaP nanoparticles was approximately 1.3 times higher than that over the Ag(5.225 wt%)/GaP nanoparticles at a time t after the start of the reaction, as shown in Fig. 6.

Conclusions

The GaP and Ag/GaP nanoparticles show high activity to degrade crystal violet in aqueous solution under visible light irradiation. It has been observed from the experimental results that the small size and low number density of Ag deposits on GaP has enhanced photocatalytic efficiency, demonstrating the effectiveness of Ag(1.139 wt%)/GaP photocatalysts in increasing the rate of photoinduced electron transfer to O_2 by electron trapping at the sites of the Ag clusters and nanoparticles. However, as the size and number density of Ag deposits on GaP increase, the recombination of photoinduced charged carriers is regarded as more competitive with processes leading to degradation of organic species.

The photocatalytic activity of the GaP and Ag/GaP nanoparticles is currently limited to the degradation of crystal violet in aqueous solution. Comparison between the

photocatalytic efficiency of the GaP and Ag/GaP nanoparticles with other similar ones is an interesting problem requiring further research. On the other hand, an interesting application of the Ag/GaP nanoparticles is its use in water splitting under visible light irradiation to evolve H_2 from aqueous solution containing sacrificial reagents. To investigate issues in exploring such photocatalytic activities is among the future research goals.

References

1. Humphreys RG, Rössler U, Cardona M (1978) Phys Rev B 18(10):5590
2. Dean PJ, Kaminsky G, Zetterstrom RB (1967) J Appl Phys 38(9):3551
3. Tsay JF, Mitra SS, Bendow B (1974) Phys Rev B 10(4):1476
4. Micic OI, Sprangé JR, Curtis CJ et al (1995) J Phys Chem 99(19):7754
5. Shi WS, Zheng YF, Wang N et al (2001) J Vac Sci Technol B 19(4):1115
6. Tang CC, Fan SS, de la Chapelle ML et al (2000) Adv Mater 12(18):1346
7. Chen LY, Luo T, Huang MX et al (2004) Solid State Commun 132(10):667
8. Cui DL, Pan JQ, Zhang ZC et al (2000) Prog Crystal Growth Charact Mater 40(1):145
9. Kim JR, Kim BK, Lee JO et al (2004) Nanotechnology 15(11):1397
10. Tsai JS, Chen FR, Kai JJ et al (2004) J Appl Phys 95(4):2015
11. Wu Q, Hu Z, Liu C et al (2005) J Phys Chem B 109(42):19719
12. Kimberly AD, Knut D, Thomas MS et al (2004) J Crystal Growth 272(1):131
13. Seo HW, Bae SY, Park J et al (2003) Chem Phys Lett 378(3–4):420
14. Han DS, Bae SY, Seo HW et al (2005) J Phys Chem B 109(19):9311
15. Kang DH, Ko JH, Bae EJ et al (2004) J Appl Phys 96(12):7574
16. Sadeghi M, Liu W, Zhang T-G, Stavropoulos P, Levy B (1996) J Phys Chem 100(50):19466

17. Litter MI (1999) *Appl Catal B* 23(2–3):89
18. Arabatzis IM, Stergiopoulos T, Bernard MC, Labou D, Neophytides SG, Falaras P (2003) *Appl Catal B* 42(2):187
19. Hirakawa T, Kamat PV (2005) *J Am Chem Soc* 127(11):3928
20. Elahifard MR, Rahimnejad S, Haghghi S, Gholami MR (2007) *J Am Chem Soc* 129(31):9552
21. Awazu K, Fujimaki M, Rockstuhl C, Tominaga J, Murakami H, Ohki Y, Yoshida N, Watanabe T (2008) *J Am Chem Soc* 130(5):1676
22. Hu C, Lan YQ, Qu JH, Hu XX, Wang AM (2006) *J Phys Chem B* 110(9):4066
23. Zhang Z-C, Zhang Q-X (2010) *J Nanopart Res* 12(3):961
24. Zhang ZC, Zhang N (2010) *Rare Metals* 29(6):561
25. Zhang Q-X, Zhang Z-C, Wang B-P (2008) *J Phys D* 41(18):185403
26. Zhang Q, Zhang Z, Zhou Z (2008) *Appl Phys B* 93(2–3):589
27. Kuhn J, Korder S, Arduini-Schuster MC, Caps R, Fricke J (1993) *Rev Sci Instrum* 64(9):2523
28. Burger T, Ploss HJ, Kuhn J, Ebel S, Fricke J (1997) *Appl Spectrosc* 51(9):1323
29. Morrison SR (1980) *Electrochemistry or semiconductor and oxidized metal electrodes*. Plenum Press, New York
30. Hotop H, Lineberger WC (1985) *J Phys Chem Ref Data* 14(3):731
31. Dweydari AW, Mee CHB (1973) *Phys Status Solid A* 17(1):247
32. Gerisher H, Heller A (1991) *J Phys Chem* 95(13):5261